Optical Engineering

SPIEDigitalLibrary.org/oe

Detection of explosives by differential hyperspectral imaging

Thierry Dubroca
Gregory Brown
Rolf E. Hummel

SPIE

Detection of explosives by differential hyperspectral imaging

Thierry Dubroca,* Gregory Brown, and Rolf E. Hummel
University of Florida, Materials Science Department, Rhines Hall, Gainesville, Florida 32611

Abstract. Our team has pioneered an explosives detection technique based on hyperspectral imaging of surfaces. Briefly, differential reflectometry (DR) shines ultraviolet (UV) and blue light on two close-by areas on a surface (for example, a piece of luggage on a moving conveyer belt). Upon reflection, the light is collected with a spectrometer combined with a charge coupled device (CCD) camera. A computer processes the data and produces in turn differential reflection spectra taken from these two adjacent areas on the surface. This differential technique is highly sensitive and provides spectroscopic data of materials, particularly of explosives. As an example, 2,4,6-trinitrotoluene displays strong and distinct features in differential reflectograms near 420 and 250 nm, that is, in the near-UV region. Similar, but distinctly different features are observed for other explosives. Finally, a custom algorithm classifies the collected spectral data and outputs an acoustic signal if a threat is detected. This paper presents the complete DR hyperspectral imager which we have designed and built from the hardware to the software, complete with an analysis of the device specifications. [DOI: 10.1117/1.OE.53.2.021112]

Keywords: explosives detection; spectroscopy; ultraviolet.

Paper 131145SS received Jul. 31, 2013; revised manuscript received Dec. 19, 2013; accepted for publication Dec. 30, 2013; published online Feb. 5, 2014.

1 Introduction and Experimental Procedure

1.1 *Hardware*

We have developed over the last few years a device based on differential reflectometry (DR) which is capable of detecting explosive materials on surfaces such as luggage, parcels, shoes, garments, etc. from a distance.[1] The DR (Ref. 1) measures the normalized difference between the reflectivities of two adjacent parts of the same specimen or two slightly different samples. Ultraviolet (UV) and blue light are shone on a surface, for example, on a piece of luggage situated on a moving conveyer belt. Upon reflection, the light is collected then diffracted by a spectrometer and its intensity recorded with a charge coupled device (CCD) camera. A computer processes the resulting data and produces in turn a differential reflection spectrum. This differential technique is highly sensitive and provides spectroscopic data of materials, specifically of explosives. As an example, 2,4,6-trinitrotoluene (TNT) displays strong and distinct features in differential reflectograms near 420 nm, that is, at the edge of the UV and visible region of the light spectrum.[2] Similarly, but distinctly different features are observed for other explosives, whereas nonexplosives display essentially no structure in the pertinent wavelength region (280 to 450 nm).[3] We have developed an improved hardware specifically designed for the fast detection of explosives on surfaces such as luggage for airport security or parcels for air shipping.

DR (also known as differential reflection spectroscopy) is a surface analytical technique that uses visible and UV light as a probing medium to reveal details about the electronic structure. In other words, the instrument detects the energies that electrons absorb from photons as they are raised into higher, allowed quantum (energy) states. Since each material has a specific electronic structure, the measurement of the characteristic energies for "electron transitions" serves as a fingerprint for identifying these substances. The differential reflectivity, which is proportional to the complex dielectric constant[1] as a function of wavelength, is unique to each material, making DR a viable investigative tool in materials science and particularly to explosives.

A number of different designs for a DR device are conceivable. For example, the object to be investigated is moved (on a conveyor belt for airport baggage scanning) and two reflectivities R_1 and R_2 are measured milliseconds apart (see Fig. 1). A broadband light source (Energetiq EQ99), 200 to 500 nm, is focused on the exterior of the luggage to be scanned due to a quartz collecting lens (50.8 mm diameter and 60 mm focal length) combined with a flat aluminum mirror (set at 90 deg) and a quartz focusing cylindrical lens (30 mm length, 20 mm width, and 25 mm focal length). The projected line, which is perpendicular to the direction of the scan as shown in Fig. 1, is 600 mm long by 3 mm wide on the conveyor belt. The focusing optics is located at 450 mm above the conveyor belt. Since the beam is diverging from the lens downward, at midheight (where the top of the luggage is located) the beam is about 300×3 mm^2.

A custom-designed spectrograph (f-number of 3) which includes a custom design collection optics (a three-mirror fold system matching the f-number of the spectrograph with a primary mirror of about 10×40 mm) made by Horiba Jobin-Yvon coupled with an UV CCD camera (Sarnoff CAM512UV, 512×512 pixels, 10×10 mm sensor size, 10 to 400 frames/s, quantum efficiency >50% over the range of interest, i.e., 250 to 450 nm) collects the reflected photons. Since there are 512 pixels along the scanning line, at midheight (i.e., on the top of the luggage) each scanning

*Address all correspondence to: Thierry Dubroca, E-mail: dubroca@gmail.com

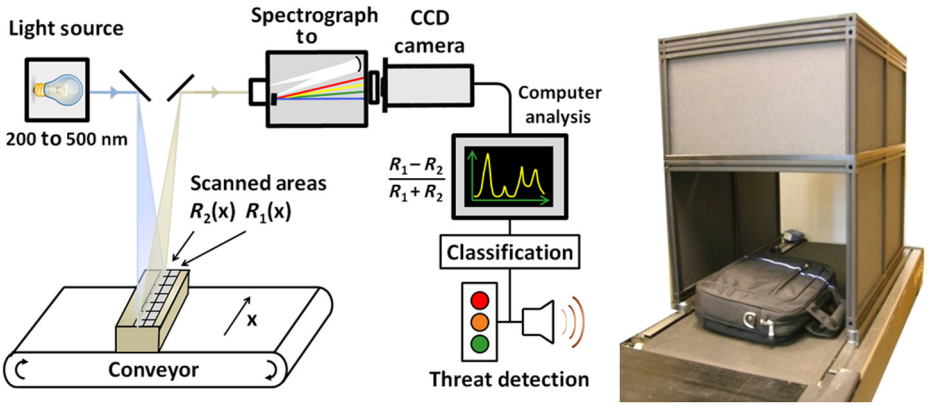

Fig. 1 Schematic representation of the differential reflectometry scanner (a). Picture of an actual device scanning a bag (b). (Adapted with changes from Ref. 4.)

pixel is 0.58×3 mm. Our custom analysis software analyzes and classifies the signal which outputs an acoustic and visual indicator if traces of explosive are detected.

1.2 *Spectral Data*

Figure 2(a) depicts characteristic spectral features for C4 (91% RDX [1,3,5-trinitroperhydro-1,3,5-triazine] and 9% plasticizer, binder, and oil), TNT, penta-erythritol tetranitrate (PETN), and ANFO (94% ammonium nitrate and 6% diesel fuel). It can be observed that each type of explosive has a different critical energy range for optical absorption, that is, PETN, ANFO, C4, and TNT have absorption edges at 290, 335, 340, and 420 nm, respectively. These absorption edges have different center wavelengths and different full widths from one another, therefore, the differential reflectograms allow us to distinguish each explosive (see below differentiation algorithm). The origin of the absorption edges stem from electronic transitions which are observed due to hydrogen bonds between explosive molecules in condensed state.[5] Without hydrogen bonds, the energy levels are different and the absorption edges listed above are not observed. Figure 2(b) displays DR spectra of white powder materials (flour, Splenda, and salt) which are similar in physical appearance to explosives but have substantial different spectral features which allows one to distinguish them from one another. Additionally, Fig. 2(b) displays the DR spectra of a red jacket and denim jeans as examples of background materials on which explosives residue can be found. The explosives spectral fingerprints are also clearly different than these background clothes.

The quality of the spectral fingerprints (shown in Fig. 2) is hardware dependent. That is, the signal-to noise-ratio depends on hardware parameters. Most of these parameters are set by the manufacturer. For example, the read-out noise from the detection camera or the light source power, fixed at 20 W, imposes a fixed number of photons interacting with the sampled surface and a given noise floor for any sample. The most important adjustable parameters are the acquisition time and the scanning speed. Figure 3 displays DR spectra of TNT measured with acquisition times ranging from 5 to 100 ms (corresponding to 200 and 10 frames/s, respectively). It is observed that the relative noise level increases as the acquisition time decreases. Furthermore, when plotting the signal-to-noise ratio as a function of the acquisition time a linear relationship is observed with a correlation coefficient of 0.82, see Fig. 4. Note that the signal is taken to be equal to the absorption edge amplitude.

The other important adjustable parameter is the conveyor scanning speed. Fig. 5(a) shows DR spectra of TNT for

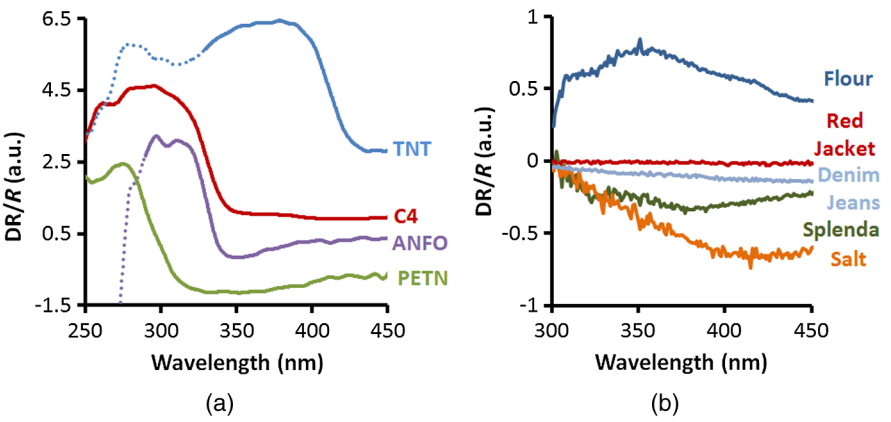

Fig. 2 (a) Differential reflectograms of some common explosive materials (TNT, C4, ANFO, and PETN). (b) Differential reflectograms of various nonexplosive materials (white powders: flour, Splenda, salt, and typical background materials, such as a red jacket and denim jeans).

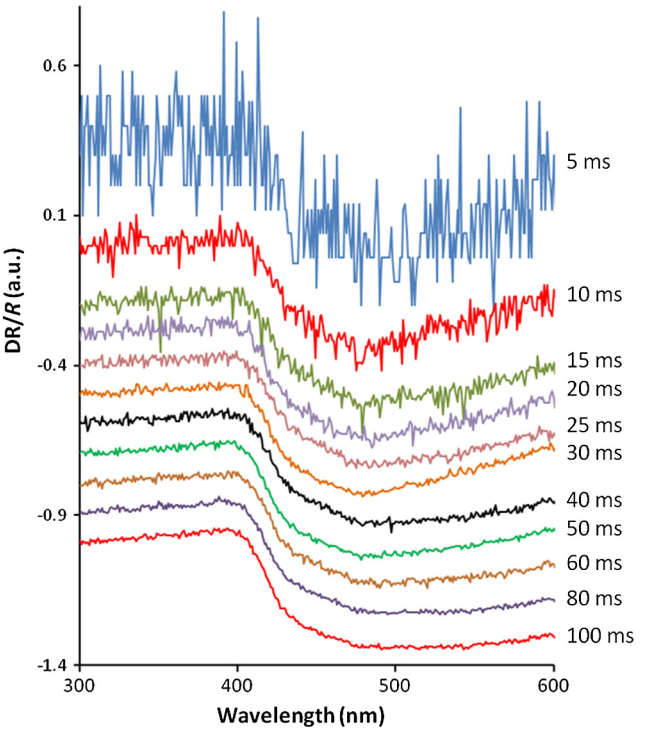

Fig. 3 Unfiltered differential reflectograms of TNT at various acquisition times (equal to one over frame rates). The curves have been shifted upward for clarity.

various scanning speeds ranging from 10 to 30 cm/s. This range is limited by the electro-mechanical design of the conveyor. Figure 5(b) displays the signal intensity of the TNT absorption edge as a function of the scanning speed. A linear trend is observed with a correlation coefficient of 0.81. This result is counter intuitive. We would expect that for a faster scanning speed the signal strength would decrease since the amount of time an explosive threat is exposed to the light beam drives the device's response. The shorter the amount of exposure time, the smaller the signal should be. But the opposite is observed. This is explained by the fact that the scanning range which we use is narrow. In this range, the signal strength is correlated with the camera frame rate. If we could expand the scanning range we would expect a result closer to our intuition. For high speeds, explosive residues on the suitcase being scanned would have a short interaction time with the light beam and therefore would generate a small signal intensity. On the other hand, for a low speed, the explosive residues would be measured in two consecutive frames and therefore

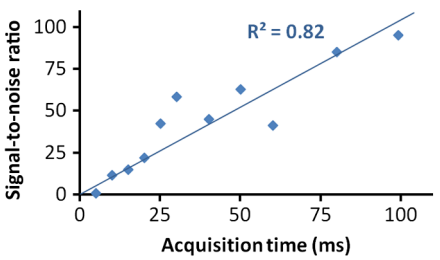

Fig. 4. Signal-to-noise ratio for a given TNT sample as a function of the acquisition time. A linear trend is observed with a correlation coefficient of 0.82. No filter was applied.

when we calculate the differential reflectivity, a smaller signal would be observed. In other words, the signal strength is dependent on the difference in reflectivities between the two parts being measured. For similar materials, the difference is small whereas for dissimilar materials, the difference is large.

In summary, the acquisition time and scanning speed have both a strong influence on the signal-to-noise ratio. The signal-to-noise ratio has an impact on the limit of detection. False positive rates and true positive rates of detection will be discussed in a later section.

2 Algorithm: Data Processing

The software design flow, as shown in Fig. 6, can be categorized into four main stages, and is executed on each frame from the UV camera. The algorithm processes frame by frame, but the calculation is done line by line (each line corresponds to an individual spectrum). The stages of the software are noise reduction, normalization, dimensional reduction, and classification. We have detailed a similar process in the previous work for TNT.[6] This section aims to extend that process with some performance improvements and additional explosives (or precursor) to the database of threats automatically detected, namely AN, PETN, and C4. We have found that due to the similarity in features, as shown in Fig. 2, the classification process is almost identical for these explosive materials.

The first step of the algorithm is to process each spectrum with a low-pass filter to remove the high frequency spectral noise. The filtered spectrum is then cropped in a second step based on the location of the significant feature to be used for the identification of each given explosive. This cropping serves to reduce the dimensionality of the data for algorithm training and increases the performance of the classification stage as well as reduces the computational time. For example, the C4 spectra were cropped between the wavelengths of 260 and 360 nm, the PETN spectra were cropped between 210 and 360 nm, and finally, the AN spectra were cropped between 290 and 390 nm. These wavelength ranges were determined through feature observation and optimized from experimental classification results. Next, each spectrum was normalized in a third step so that the amplitude covers the range between 0 and 1. The purpose of the normalization is to account for the wide range of amplitudes that are observed from different amounts of explosives in a given spectrum. The noise in the spectrum, although reduced through filtering, is amplified by the normalization. Therefore, a second round of noise reduction is applied in a fourth step. This preclassification processing ensures maximal performance of the classification stage.

We use principal component analysis (PCA) to reduce dimensionality further, projecting each spectrum onto the five most significant eigenvectors.[6] PCA is implemented identically for all explosives. The result of this process is the reduction of a 150-point spectrum into a 5-point vector, making real-time classification feasible. This stage can be seen in the design flow in Fig. 6 as "dimensional reduction."

The current classification methodology for determining the presence of explosives on a surface is based on support vector machines (SVM). The SVM algorithm[6–8] is a classifier that finds a hyperplane in the kernel space that maximizes the margin between explosive and nonexplosive

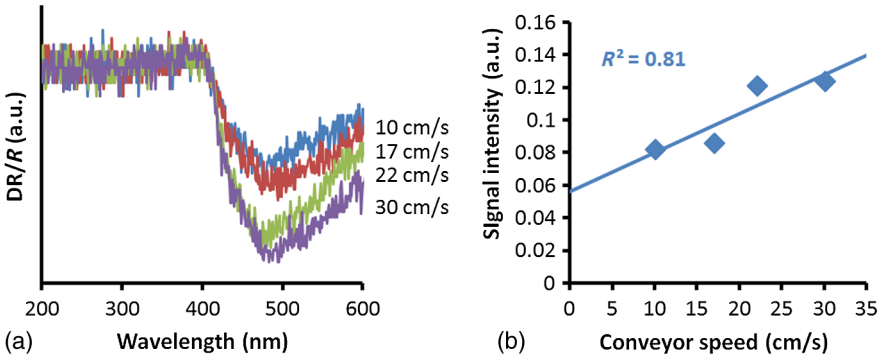

Fig. 5 Differential reflectograms of TNT for various conveyor scanning speeds (a). Signal-to-noise ratio of a given TNT sample as a function of the conveyor speed (b). The acquisition time was 10 ms for all measurements and no filter was applied.

spectra. We found this pattern recognition algorithm to be the most suitable for our application.

SVM classifiers were trained for each explosive to maximize our ability to identify threat and nonthreat samples. The general composition of each data set was thousands of nonexplosive spectra and hundreds of explosive spectra. A 10-fold cross-validation process was used to determine the performance of the classifier, in which the explosive and nonexplosive samples are split evenly into 10 subsets. The purpose of the 10-fold analysis is to remove bias from any particular subset of the data. Nine of the 10 subsets are used for training and one for verification. This process is repeated 10 times for each subset, resulting in a complete analysis of the classifiers generated.[9]

3 Implementation and Optimization of Processing Algorithm

The application of our explosive detection technique requires an implementation with real-time performance. The real-time performance requires that the data be processed faster than it is acquired. In addition, the system as a whole needs to detect the smallest explosive residue possible. Therefore, a tradeoff has to be found between the acquisition rate, conveyor speed, and data processing. In order to achieve a useful application performance, the algorithm was transcribed into a high performance C implementation. This implementation pays special attention to accuracy, loop unrolling for repetitive calculations, and the use of an optimized mathematical library which utilizes basic linear algebra subprograms.[10]

The implemented real-time algorithm transfers one frame of data from the camera into a memory buffer, then processes it using the detection algorithm before the next frame is acquired and transferred into the memory buffer. It is imperative that the algorithm process be faster than the camera acquisition rate so that no frame potentially containing threats is lost.

Figure 7 displays computational times executed on a Windows 7-operated computer with a Quad Core Intel Xeon W3520 processor running at 2.67 GHz with 12 GB of RAM. The implemented algorithm runs a Boolean output classifier (TNT versus nonthreat) on a full 512×512 data frame.

MATLAB runtime is used as the baseline for comparing code performances, see Fig. 7. Using "SVM Light,"[11] a versatile C implementation for training and classifying with SVM and our C code transcribed custom-designed algorithm, described above, the computational time is reduced from 120 to 30 ms/frame. This is a dramatic 4-fold speed improvement. Optimizing the SVM code to our application gained about 5 ms, reducing the per frame computational time to 25 ms. Upon further analysis of the

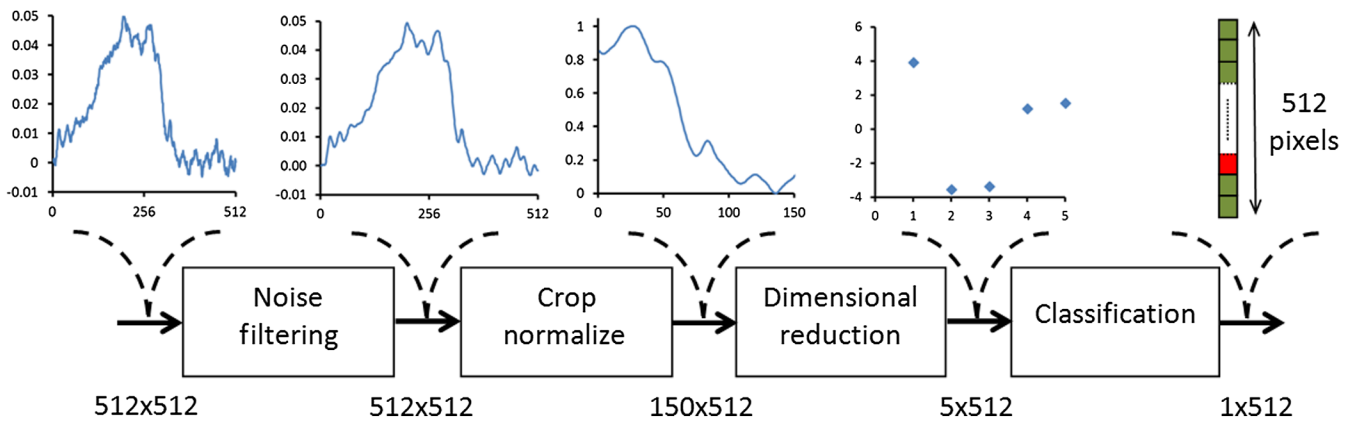

Fig. 6 Algorithm design flow. The input is a 512×512 differential image. The output is the result of classification which labels each spectrum as threat (red) or nonthreat (green), a 512 pixels long vector. Dimensions of the data are shown after each step. Typical spectra are shown at various stages of the process in the top row.

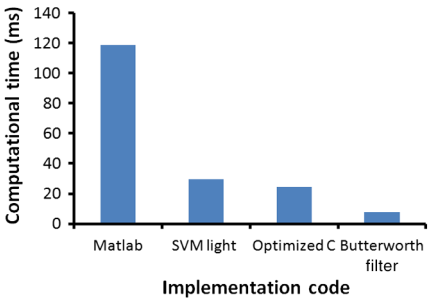

Fig. 7 Computation time as a function of the implemented code used.

individual steps in the algorithm, it was determined that the filtering stage used the majority of the computational time (about 20 ms or 75% of the optimized C implemented algorithm). This stage uses a one-dimensional median filter with a 15-pixels wide window. Such a large window size, necessary to significantly reduce the noise,[4] requires a large amount of computation. Replacing the median filter with a Butterworth filter significantly reduced the computational time another 3-fold to about 8 ms/frame, while sacrificing a relatively small amount, about 25%, of noise reduction.

The current system developed, given the 8 ms/frame computational time, allows time for 12 additional classifiers (one for each explosive) while maintaining real-time performance. In order to maximize the limit of detection[12] and the number of explosives detectable in real time, the camera frame rate is set at 10 Hz (or 100 ms/frame). If one were to increase the number of explosives to be detected at the same time or increase the frame rate major changes would be necessary. For example, the hardware use to run the algorithm would need to include the addition of a graphical processing unit (GPU). GPUs specialize in parallelized many-thread computations are known to yield large increases in speed for image processing applications.[13] Another possible approach would be to use a multicategory classifier instead of one classifier for each explosive material.

4 Detection System Performance

4.1 *Limit of Detection*

The absolute limit of detection of the present DR system was determined to be about 100 ng for TNT.[12] Briefly, the limit of detection is defined as the mass of explosive material necessary to obtain a signal-to-noise ratio of three. In a past experiment,[12] we acquired the DR spectra of TNT samples of different sizes ranging from filling a full square pixel, 0.58×3 mm (1.74 mm^2) by 4-μm thick corresponding to about 11 μg, down to filling about 1% of a pixel, a triangular shape 0.58×0.05 mm (0.0145 mm^2) by 4-μm thick[4] which is about 100 ng. In this experiment, the samples were prepared by packing a fine powder on a flat substrate. The thickness of 4 μm was determined to be an upper limit of the minimal interaction thickness between the TNT and the probing beam. Below this thickness, it becomes very difficult to control the flatness and packing of the fine TNT powder. Therefore, it is difficult to determine the minimal interaction thickness of TNT in the UV region of the spectrum. After acquiring the spectra, we extracted the signal-to-noise ratio for each sample size. We found a linear relationship between the sample size and the signal-to-noise ratio.[4] From this linear relationship, we evaluated the limit of detection as per its definition. It should be said that this definition may not always lead to a usable limit of detection. We have observed that, for the algorithm presented in the previous section, the practical limit of detection is about two times larger at about 200 ng for TNT (i.e., signal-to-noise ratio of about 5) than the absolute limit. Similar limit of detection values has been found for other explosives. It should be added that the sample shape has a very strong influence on the detection limit.[14] First, the geometry of the sample matters. Only the top 4 μm of explosive material will be sensed by the scanning beam. Therefore, detecting thick samples will increase the detection limit. Second, the roughness was found to have a strong influence on the reflectivity of the sample[14] and as a consequence has an effect on the limit of detection. The DR is most sensitive for strongly diffusive and weakly specular samples, that is, for rough rather than smooth sample surfaces. Real threats, such as explosive residues in the form of particles or finger prints, are thin with diffusive surfaces and therefore the method presented above is of practical significance.

Future development is being considered to improve the limit of detection of DR in order to reach trace level detection. This means being able to sense a few tens of micrometer size diameter particles[15] weighing between one and a few tens of nanograms. In order to attain such sensitivity, one could increase the intensity from the light source, for example, using more efficient optics (i.e., custom designed) or a more powerful source, or increase the size of the collection optics, thus increasing the photon flux going to the camera. Our current system is only using about 10% of the dynamic range of the camera. Using 100% of the dynamic range would allow our detection system to reach a 10-ng detection limit.

Other standoff optical techniques have been applied to explosive detection by hyperspectral imaging. In particular, Raman [deep UV[16]and coherent anti-Stokes Raman spectroscopy[17]] and short-wave infrared[18] have been developed to detect nanogram range threats, however, these techniques suffer from slow scanning speed and they cannot at the present time handle large surface screening at these detection levels. On the other hand, DR is about two orders of magnitude faster with the ability to screen the top surface of carry-on size luggage in about 3 s.

In addition to the limit of detection, the performance of a detection system is evaluated by its capacity to differentiate threats and nonthreats. Such performance is evaluated using receiver operating characteristic (ROC) curves which display the true positive rate as a function of the false positive rate for any detection system.

4.2 *ROC Curves*

The ROC curves for each explosive are displayed in Fig. 8. These results were generated for each classifier (i.e., each explosive individually). The classifiers were trained for each explosive as described in Sec. 2. For each explosive, two different data sets were used to train the classifiers and therefore generated two ROC curves. In the first case, the data set contains explosives spectra of sample sizes ranging from about 0.03 to 100 μg. That is from below the limit of detection to above the maximum dynamic range of our system. In the second case, the data set contains only explosives spectra with

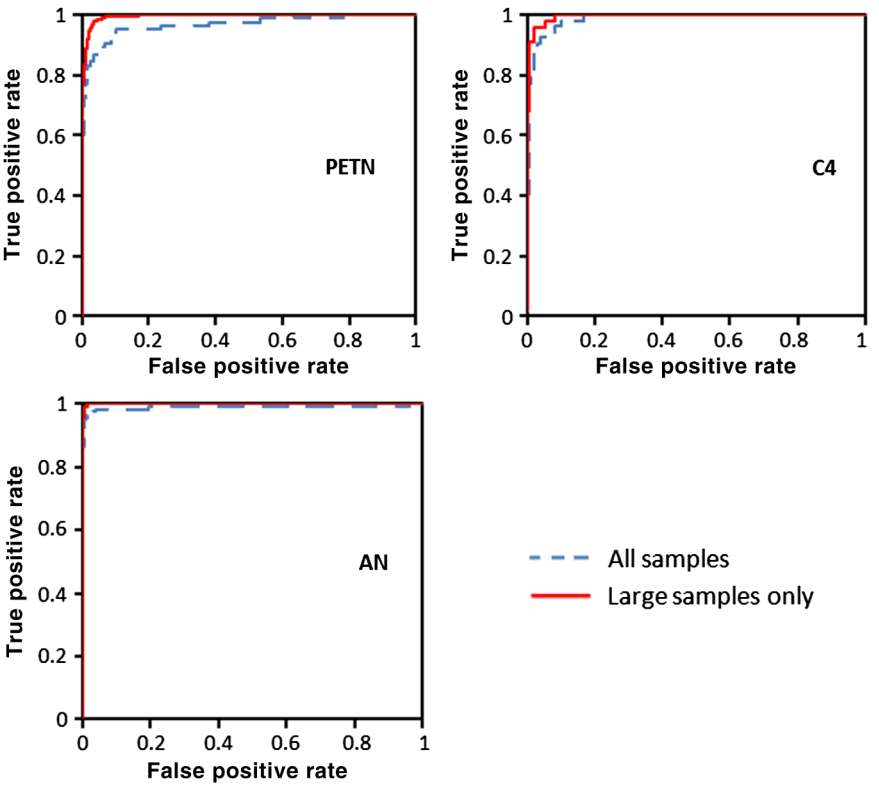

Fig. 8 Receiver operating characteristic curves of three materials: PETN, C4, and AN. The curves labeled "All samples" represent the classifier trained with every explosives sample in the set, sample sizes range from 0.03 and 100 μg (0.3% and above fill factor). The curves labeled "Large samples only" represent the classifier trained without the samples close to or below the limit of detection. Large sample sizes range between 0.2 and 100 μg (2% and above fill factor).

SNR above 5 (sample sizes ranging from 0.2 to 100 μg), which is above twice the limit of detection. Removing samples near the limit of detection have a small effect on the system performance. For example, in the case of C4, at 5% false positive rate, the true positive rate increases only by 0.05 (from 0.92 to 0.97). This demonstrates that the robustness of the algorithm developed is in the 0.2 to 100 μg range.

Figure 8 displays a good performance of the detection system as long as the sample size is above about 0.2 μg (SNR = 5). Below this value, the classification algorithm loses its ability to differentiate explosives from nonexplosives materials due to noise confusion. That is, the algorithm detects noise where the spectral features of explosives are normally located which causes a dramatic increase in the false positive rate.

The data set of each explosive varied in regards to the number of explosive and nonexplosive samples used in training. PETN was trained with 30,000 non-PETN samples and 825 PETN samples. C4 was trained with 14,000 non-C4 samples and 520 C4 samples. AN was trained using 20,000 non-AN samples and 1200 AN samples. Approximately 10% of each explosives sample sets was comprised of samples near the limit of detection and was removed to demonstrate the difference shown in Fig. 8. The nonexplosives samples were generally comprised of clothing materials of different compositions and colors.[9]

5 Conclusions

This study demonstrates that various explosive substances, such as TNT, RDX, C4, PETN, and AN can be identified with good accuracy down to the low microgram range by applying differential reflection spectroscopy. This standoff technique is fast, eye safe (no laser light or X-ray), automatic, and does not require human involvement. For the data processing, an algorithm has been developed which involves noise reduction by filtering, cropping, and normalization. For each explosive substance, two different data sets were used to train the classifiers and to generate the ROC curves. ROC curves yield true positive rates in the range of 97%.

References

1. R. E. Hummel, "Differential reflectance spectroscopy in analysis of surfaces," in *Encyclopedia of Analytical Chemistry*, R. A. Meyers, Ed., pp. 9047–9071, Wiley, Chichester (2000).
2. R. E. Hummel et al., "Detection of explosive materials by differential reflection spectroscopy," *Appl. Phys. Lett.* **88**(23), 231903 (2006).
3. C. Schöllhorn et al., "Developments on standoff detection of explosive materials by differential reflectometry," *Appl. Opt.* **46**(25), 6232–6236 (2007).
4. T. Dubroca, K. Vishwanathan, and R. E. Hummel, "The limit of detection for explosives in spectroscopic differential reflectometry," *Proc. SPIE* **8018**, 80181L (2011).
5. T. Dubroca, K. Moyant, and R. E. Hummel, "Ultra-violet and visible absorption characterization of explosives by differential reflectometry," *Spectrochim. Acta A* **105**, 149–155 (2013).
6. S. E. Yuksel et al., "An automatic detection software for differential reflection spectroscopy," *Proc. SPIE* **8390**, 83900B (2012).
7. S. E. Yuksel et al., "Differential reflection spectroscopy: a novel method for explosive detection," *Acta Phys. Pol. A* **123**(2), 263–264 (2013).
8. C. M. Bishop, *Pattern Recognition and Machine Learning (Information Science and Statistics)*, Springer-Verlag, New York (2006).
9. S. E. Yuksel et al., "Spectral analysis for the detection of explosives with differential reflectometry," in *Proc. Grace Hopper Celebration for Women in Computing*, Portland, Oregon, Vol. 1, p. 46 (2011).

10. L. S. Blackford et al., "An updated set of basic linear algebra subprograms (BLAS)," *ACM Trans. Math. Software* **28**(2), 135–151 (2002).
11. T. Joachims, "Making large-scale SVM learning practical," in *Advances in Kernel Methods—Support Vector Learning*, B. Schölkopf, C. Burges, and A. Smola, Eds., pp. 169–184, MIT, Cambridge, Massachusetts (1999).
12. T. Dubroca and R. E. Hummel, "Detection of explosives by hyperspectral differential reflectometry," in *Proc. of Materials Research Society*, Vol. 1405 (2011).
13. J. D. Owens et al., "GPU computing," *Proc. IEEE* **96**, 879–899 (2008).
14. T. Dubroca, G. Guetard, and R. E. Hummel, "Influence of spatial differential reflection parameters on 2,4,6-trinitrotoluene (TNT) absorption spectra," *Proc. SPIE* **8358**, 83581Y (2012).
15. J. R. Verkouteren, "Particle characteristics of trace high explosives: RDX and PETN," *J. Forensic Sci.* **52**(2), 335–340 (2007).
16. R. Bhartia, W. F. Hug, and R. D. Reid, "Improved sensing using simultaneous deep UV Raman and fluorescence detection," *Proc. SPIE* **8358**, 83581A (2012).
17. A. Dogariu and A. Pidwerbetsky, "Coherent anti-stokes Raman spectroscopy for detecting explosives in real-time," *Proc. SPIE* **8358**, 83580R (2012).
18. M. R. Papantonakis et al., "Stand-off detection of trace explosives by infrared photothermal imaging," *Proc. SPIE* **7304**, 730418 (2009).

Thierry Dubroca received his undergraduate degree in engineering physics from Grenoble Institute of Technology in France. Then received his MS and PhD from University of Florida Materials Science and Engineering Department. After PhD he worked on developing the technology associated with explosive detection by differential reflectometry. Recently, he took a postdoctoral position at the National High Magnetic Field Laboratory where he is developing a new type of nuclear magnetic resonance system called dynamic nuclear polarization.

Gregory Brown graduated from University of Florida in 2012 with a Master of Science in electrical engineering. He had a particular interest in high speed computing (hardware and software). Since graduation he has been involved in the development of a high-speed algorithm for real-time detection of explosives.

Rolf E. Hummel is an emeritus professor in the Materials Science and Engineering Department at the University of Florida. He has 50 years of experience in the field of electronic materials, particularly in optoelectronics. He has written a widely used textbook on this subject that is now in its fourth edition, and has authored a monograph on optical properties of metals and alloys. He has published 190+ research papers in refereed international journals and has been an invited speaker for numerous, prestigious international conferences.